π-Dimers of Prototype High-Spin Polaronic Oligomers

John A. E. H. van Haare, Marc van Boxtel, and René A. J. Janssen*

Laboratory of Organic Chemistry, Eindhoven University of Technology, P.O. Box 513, 5600 MB Eindhoven, The Netherlands

Received November 18, 1997. Revised Manuscript Received February 6, 1998

Novel well-defined oligomers consisting of two dopable π-conjugated segments, 2,2′-bipyrrole or 2,2′-bithiophene, linked via 1,3-phenylene and end-capped with phenyl groups have been synthesized using palladium-catalyzed cross-coupling reactions. The molecules are considered as prototypical examples for polaronic ferromagnetic chains based on pyrrole and thiophene units, which have been proposed as candidates for organic magnetic materials. The oligomers are designed to investigate whether high-spin (i.e. triplet-state) oligocations can be obtained after oxidative doping. We find that the oligomers can be oxidized to the corresponding di(cation radical)s, in which each heterocyclic segment is singly oxidized and carries an unpaired electron, as required for a high-spin state. While these di(cation radical)s are stable at ambient temperature, UV/visible/near-IR and ESR spectroscopy reveals that the singly charged cation radical segments reversibly form π-dimers in solution, especially at low temperatures. This π-dimerization involves the intermolecular antiferromagnetic pairing of electron spins and is detrimental for the formation of high-spin oligomers or polymers via the polaronic concept with oxidized oligopyrrole or oligothiophene segments as spin-carrying units.

Introduction

The design of organic molecules and polymers with unusual magnetic properties has been the focus of much recent research.[1−7] A well-established strategy to prepare organic high-spin molecules is to connect neutral or charged π-radicals as spin-carrying units (SCUs) via organic linkers that act as a ferromagnetic coupling units (FCUs) and provide the desired alignment of electron spins. As a result, the magnetic moment of the molecule is proportional to the number of unpaired electrons. 1,3-Phenylene (*m*-phenylene) is generally considered as a versatile and fairly robust FCU. It couples radical centers at the 1 and 3 positions by an in-phase periodicity of the spin polarization of its π-electrons, imposed by the topological symmetry. Considerable interest has been directed to designing and preparing novel, preferably stable, organic radicals that can be incorporated into new high-spin systems. Cooperative interaction of a large number of unpaired electrons may eventually result in high-spin polymers [(FCU−SCU)$_n$] and ultimately ferromagnetic materials.

A particularly interesting strategy toward high-spin polyradicals, theoretically developed by Fukutome et al., is that of a polaronic ferromagnetic chain in which unpaired electrons can be introduced by reduction or oxidation of π-conjugated segments that are positioned between FCUs.[8] Redox doping of such a polymer to a high-spin state would be similar to the well-established doping of π-conjugated polymers to highly conducting materials. The possibility to employ redox reactions for obtaining high-spin molecules has been demonstrated experimentally for well-defined π-conjugated systems. Reduction of 1,3-di(1-naphthyl)benzene and oxidation of 1,3-di(9-anthryl)benzene provides triplet ground state di(ion radical)s.[9] In similar procedures, *p*-phenylenediamine oligomers linked via 1,3-phenylene and 1,3,5-benzenetriyl have been successfully oxidized to high-spin ground-state oligo(cation radical)s ($S = 1$ and $1^1/_2$), which are stable at room temperature.[10,11]

The polaronic strategy has also been applied to polymers,[12−14] incorporating 1,3-phenylene units as FCU in π-conjugated polymer chains such as polyacetylene and polythiophene, e.g.:[12,13]

(1) Gatteschi, D., Kahn, O., Miller, J. S., Palacio, F., Eds. *Magnetic Molecular Materials*; Kluwer Academic Publishers: Dordrecht, The Netherlands, 1991.
(2) Iwamura, H., Miller, J. S., Ed. *Chemistry and Physics of Molecular Based Magnetic Materials. Molecular Crystals and Liquid Crystals*; Gordon and Breach Publishers: New York, 1993; Vol. 232, pp 1−360.
(3) Miller, J. S.; Epstein, A. J. *Angew. Chem., Int. Ed. Engl.* **1994**, *33*, 385.
(4) Rajca, A. *Chem. Rev.* **1994**, *94*, 871.
(5) Iwamura, H. *Adv. Phys. Org. Chem.* **1990**, *26*, 179.
(6) Iwamura, H.; Koga, A. *Acc. Chem. Res.* **1993**, *26*, 346.
(7) Turnbull, M. M., Sugimoto, T., Thompson, L. K., Eds. *Molecule-Based Magnetic Materials: Theory, Technique, and Applications*; American Chemical Society: Washington, DC, 1996; Vol. 644.
(8) Fukutome, H.; Takahashi, I.; Ozaki, M. *Chem. Phys. Lett.* **1987**, *133*, 34.
(9) Tukada, H. *J. Chem. Soc., Chem. Commun.* **1994**, 2293.
(10) (a) Wienk, M. M.; Janssen, R. A. J. *J. Am. Chem. Soc.* **1997**, *119*, 4492. (b) Wienk, M. M.; Janssen, R. A. J. *J. Am. Chem. Soc.* **1996**, *118*, 10626. (c) Wienk, M. M.; Janssen, R. A. J. *Chem. Commun.* **1996**, 267.
(11) (a) Stickley, K. R.; Blackstock, S. C. *J. Am. Chem. Soc.* **1994**, *116*, 11576. (b) Stickley, K. R.; Selby, T. D.; Blackstock, S. C. *J. Org. Chem.* **1997**, *62*, 448.
(12) Kaisaki, D. A.; Chang, W.; Dougherty, D. A. *J. Am. Chem. Soc.* **1991**, *113*, 2764.
(13) Murray, M. M.; Kaszynski, P.; Kaisaki, D. A.; Chang, W.; Dougherty, D. A. *J. Am. Chem. Soc.* **1994**, *116*, 8152.
(14) Bushby, R. J.; Ng, K. M. *Chem. Commun.* **1996**, 659.

S0897-4756(97)00759-X CCC: $15.00
Published on Web 03/28/1998

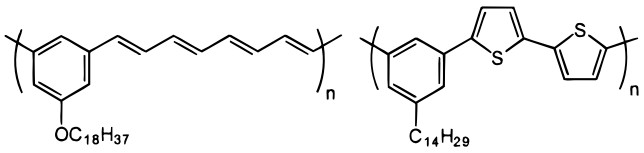

Oxidation of these tailor-made polymers was found to give rise to net ferromagnetic coupling of spins along the chain, as determined by fitting the normalized experimental (low-temperature) magnetization to the Brillouin function for different values of S, yielding $S > {}^1/_2$. Surprisingly, however, the spin concentration in these polaronic polymer chains was extremely low. Only a few percent of the doped monomers units actually carried an unpaired electron.[12−14] In order to rationalize the $S > {}^1/_2$ values in combination with the low spin concentration, it has been proposed that inhomogeneous doping occurs, resulting in heavily doped islands that produce large S values.[13]

Previous investigations have shown that pyrrole and thiophene oligomers, when protected at the α-positions, can be quantitatively oxidized to the corresponding cation radicals, which are stable at ambient temperature.[15−17] This makes these units interesting candidates to achieve high-spin oligomers, via the polaronic concept. On the other hand, it is has been firmly established that cation radicals of oligopyrroles and oligothiophenes can form diamagnetic π-dimers in the solid state and in solution at low temperatures.[15−17] Obviously, π-dimerization and the associated antiferromagnetic pairing of unpaired electrons would be detrimental for obtaining high-spin molecules or polymers via the polaronic chain concept. Alternatively, this might offer an explanation to the low spin concentration found for polaronic ferromagnetic chains up to now.[12−14]

In order to investigate the polaronic strategy in more detail and to assess the possible role of π-dimerization, we set out to prepare and study oligomers consisting of two dopable π-conjugated segments, based on pyrrole and thiophene oligomers, linked via 1,3-phenylene as FCU (Figure 1). In designing prototype high-spin oligomers **1** and **2**, we restricted the π-conjugated segments to two heterocyclic rings. The rationale for this choice was the expectation that the limited dimension of the π-segments reduces the extent of delocalization of charge and spin after doping and thereby enhances the unpaired electron density at the carbon atoms directly connected to the central 1,3-phenylene ring, which is favorable for achieving strong ferromagnetic coupling. A further reduction of the π-dopable segment to only one heterocyclic ring is not feasible, since it would result in too high of oxidation potentials and a loss of chemical stability of the cation radicals produced in the oxidation reaction. Here, we describe the preparation, redox behavior, and tendency to form π-dimers of the prototype high-spin oligomers **1** and **2,**

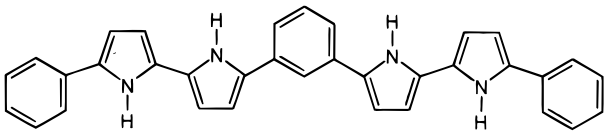

1

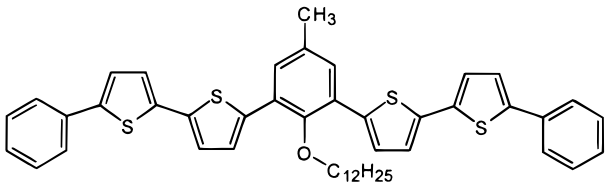

2

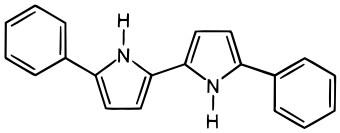

3

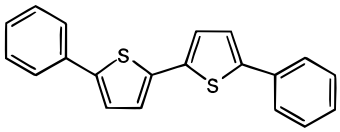

4

Figure 1. Precursors to prototype high-spin polaronic oligomers based on bipyrrole and bithiophene (**1**, **2**) and their model compounds (**3**, **4**).

and compare the results with those of compounds **3** and **4** that contain only one dopable π-segment (Figure 1).

Results and Discussion

Synthesis. The synthesis of compounds **1**−**4** was accomplished using Stille reactions, involving palladium-catalyzed cross-couplings of arylstannanes with arylhalides. The preparation of 5,5′-diphenyl-2,2′-bipyrrole **3** has been described previously.[18] 5,5′-Diphenyl-2,2′-bithiophene **4** was prepared in 65% yield by reacting 5,5′-dibromo-2,2′-bithiophene[19] with trimethylstannylbenzene in a mixture of toluene and an aqueous Na_2CO_3 solution (1 M) using tetrakis(triphenylphosphine)-palladium(0) as a catalyst.

The synthesis of compound **8**, as a direct precursor to **1**, carrying *N*-*tert*-butoxycarbonyl protective groups, is outlined in Scheme 1. 1,3-Dibromobenzene was coupled with 2 equiv of *N*-*tert*-butoxycarbonyl-2-(trimethylstannyl)pyrrole[20] in a palladium(0)-catalyzed Stille reaction. After purification and recrystallization, this afforded 1,3-bis(*N*-*tert*-butoxycarbonyl-2-pyrrolyl)-benzene **5** in 50% yield. The occurrence of an exchange reaction involving the aryldibromide and the trimeth-

(15) (a) Hill, M. G.; Mann, K. R.; Miller, L. L.; Penneau, J.-P. *J. Am. Chem. Soc.* **1992**, *114*, 2728. (b) Hill, M. G.; Penneau, J.-F.; Zinger, B.; Mann, K. R.; Miller, L. L. *Chem. Mater.* **1992**, *4*, 1106.

(16) (a) Bäuerle, P.; Segelbacher, U.; Maier, A.; Mehring, M. *J. Am. Chem. Soc.* **1993**, *115*, 10217. (b) Bäuerle, P.; Segelbacher, U.; Gaudl, K. U.; Huttenlocher, D.; Mehring, M. *Angew. Chem., Int. Ed. Engl.* **1993**, *32*, 76.

(17) van Haare, J. A. E. H.; Groenendaal, L.; Havinga, E. E; Janssen, R. A. J.; Meijer, E. W., *Angew. Chem., Int. Ed. Engl.* **1996**, *35*, 638.

(18) van Haare, J. A. E. H.; Groenendaal, L.; Peerlings, H. W. I.;. Havinga, E. E; Vekemans, J. A. J. M.; Janssen, R. A. J.; Meijer, E. W. *Chem. Mater.* **1995**, *7*, 1984.

(19) Bäuerle, P.; Würther, F.; Götz, G.; Effenberger, F. *Synthesis* **1993**, 1099.

(20) Martina, S.; Enkelmann, V.; Schlüter, A.-D.; Wegner, G. *Synthesis* **1991**, 613.

Scheme 1. Synthesis of 1: (a) $Pd^0(PPh_3)_4$, Toluene/Water (1 M Na_2CO_3, 1:1 v/v), 100 °C; (b) NBS, THF, −70 °C; (c) $Pd^0(PPh_3)_4$, Toluene/Water (1 M Na_2CO_3, 1:1 v/v), 100 °C; (d) Thermolysis, 190 °C

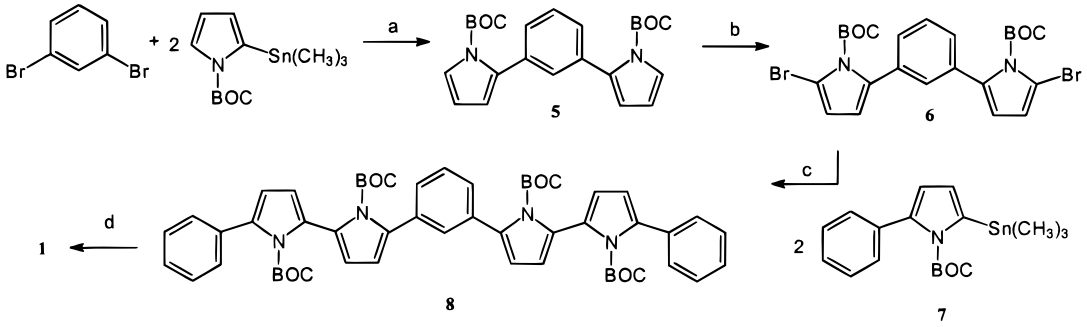

Scheme 2. Synthesis of 2: (a) (1) *n*-BuLi, THF, −70 °C, (2) $(CH_3)_3SnCl$, THF, −70 °C; (b) Bromobenzene, $Pd^0(PPh_3)_4$, Toluene/Water (1 M Na_2CO_3, 1:1 v/v), 100 °C; (c) (1) *n*-BuLi, THF, −70 °C, (2) $(CH_3)_3SnCl$, THF, −70 °C; (d) $Pd^{II}(PPh_3)_2Cl_2$, THF, Reflux

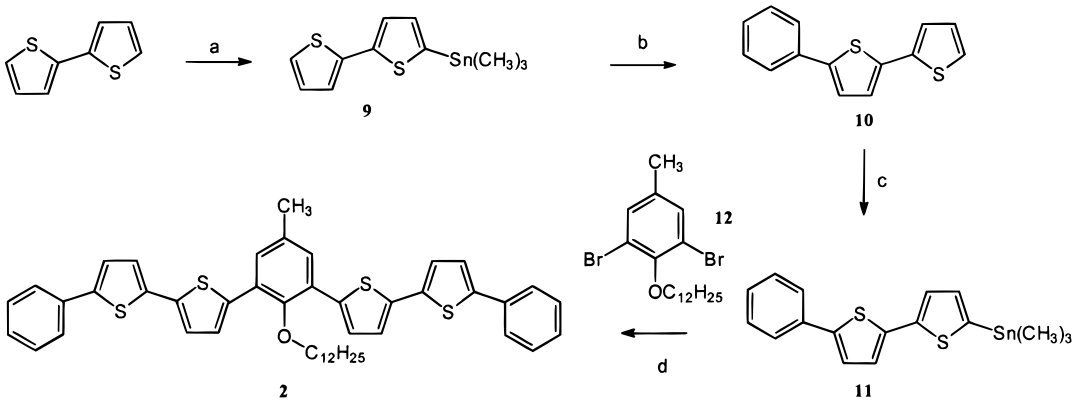

ylstannyl substituent on pyrrole, in which one bromine is replaced by a methyl group, prohibits high yields of **5** in this reaction. Subsequent bromination of the free α-pyrrole positions of **5** using *N*-bromosuccinimide (NBS) in tetrahydrofuran (THF) afforded **6** in 100% yield. Coupling of **6** with 2 equiv of *N*-*tert*-butoxycarbonyl-2-trimethylstannyl-5-phenylpyrrole **7** in toluene/aqueous Na_2CO_3 solution (1 M), using a catalytic amount of tetrakis(triphenylphosphine)palladium(0), gave after usual work-up procedures and crystallization derivative **8** in 36% yield. Field desorption mass spectrometry (FD-MS) confirmed the correct mass (890.7 amu) but also revealed a small contamination from side products due to homocoupling and debromination. Preparative HPLC (reversed phase column, eluent acetonitrile/water 9:1) gave pure **8**, which was deprotected quantitatively by thermolysis at 200 °C under vacuum, yielding pure **1**.

Compound **2**, substituted on the central 1,3-phenylene ring with a dodecyloxy group to enhance solubility, was prepared following a different reaction sequence (Scheme 2). Starting from 2,2′-bithiophene,[21] selective stannylation using *n*-butyllithium and quenching with trimethylstannyl chloride afforded 5-trimethylstannyl-2,2′-bithiophene **9** in 85% yield. Subsequent coupling with bromobenzene resulted in the formation of 5-phenyl-2,2′-bithiophene **10** (yield 50%), which was stannylated at the free α-thiophene position to give **11** in 100% yield. Reaction of 5-methyl-2-dodecyloxy-1,3-dibromobenzene **12** with **11** in refluxing THF using tetrakis(triphenylphosphine)palladium(II) chloride as a catalyst (Scheme 2) afforded compound **2,** albeit in only 10% yield after crystallization.[22] Preparative HPLC (reversed phase, eluent THF/water 3:1) was used to purify **2** from 5,5‴-diphenyl-2,2′:5′,2″:5″,2‴-quaterthiophene which was formed as a byproduct in a homocoupling reaction of compound **11.** The final sample of **2** used in this study contained a residual extent of this byproduct (2%, based on HPLC).

Cyclic Voltammetry. To investigate the redox behavior and stability of the different redox states, electrochemical measurements were performed in dichloromethane with 0.1 M tetrabutylammonium hexafluorophosphate ($Bu_4N^+PF_6^-$) as supporting electrolyte. The results are shown in Figure 2 and summarized in Table 1. Phenyl-end-capped bipyrrole and bithiophene oligomers **3** and **4** exhibit two chemically reversible one-electron oxidation waves with peak-to-peak separations between oxidation potential E_{pa} and reduction potential E_{pc} of 70−100 mV. The cation radicals $\mathbf{3}^{\bullet+}$ and $\mathbf{4}^{\bullet+}$, as well as the dications $\mathbf{3}^{2+}$ and $\mathbf{4}^{2+}$, are stable on the time scale of the cyclic voltammetry experiment. The chemical stability of the redox states is strongly enhanced by the two phenyl end caps, which prevent polymerization of the bipyrrole and bithiophene units over the otherwise free α-positions. Compound **1** also shows two chemically reversible redox waves, but now the interpretation is different. Comparison with the redox potentials of **3** reveals that, for **1**, both redox waves correspond to a two-electron process in which the di-

(21) Keegstra, M. A.; Brandsma, L. *Synthesis* **1988**, 890.

(22) Kang, B. S.; Seo, M.-L.; Jun, Y. S.; Lee, C. K.; Shin, S. C. *Chem. Commun.* **1996**, 1167.

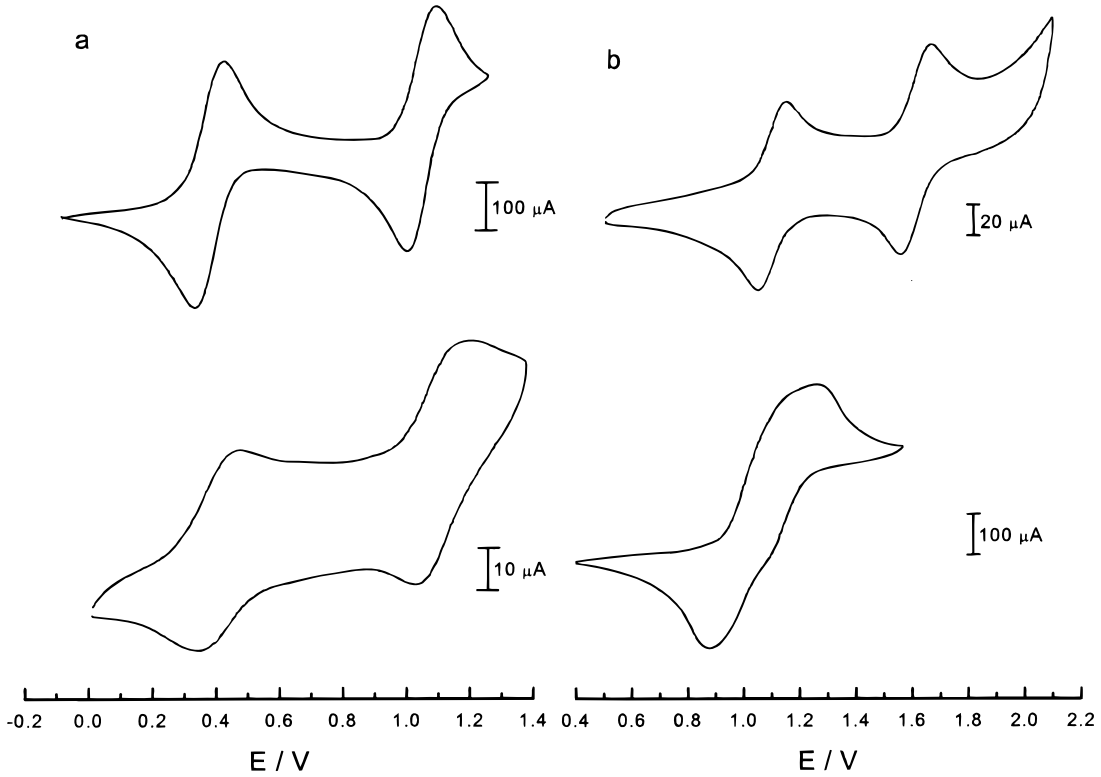

Figure 2. Cyclic voltammograms of oligomers at 295 K in dichloromethane/ $Bu_4N^+PF_6^-$ (0.1 M), scan rate 100 mV/s. (a, top) **3**; (a, bottom) **1**; (b, top) **4**; (b, bottom) **2**. Potential vs SCE calibrated against Fc/Fc^+ (0.43 V).

Table 1. Electrochemical Data of Compounds 1−4[a]

compd	E_{pa1}/E_{pc1} (V)	E_{pa2}/E_{pc2} (V)
1	0.50/0.36	1.19/1.04
2	1.13/0.88	1.26/1.09
3	0.42/0.35	1.09/1.00
4	1.14/1.06	1.66/1.56

[a]Cyclic voltammetry measurements were performed in dichloromethane with 0.1 M $Bu_4N^+PF_6^-$ as supporting electrolyte; scan rate, 100 mV/s. Potentials are referenced to SCE.

(cation radical) $\mathbf{1}^{2\bullet 2+}$ and the tetracation $\mathbf{1}^{4+}$ are formed, respectively. The peak-to-peak separations ($E_{pa}-E_{pc}$) of **1** are about 150 mV, which may be interpreted as being the consequence of two consecutive, but unresolved, one-electron oxidation waves. The cyclic voltammogram of **2** reveals two partially resolved one-electron oxidation waves centered around 1.08 V. Comparison with the first redox wave of **4** (at 1.10 V) suggests that this wave represents the process $\mathbf{2} \rightarrow \mathbf{2}^{\bullet+} \rightarrow \mathbf{2}^{2\bullet 2+}$. In contrast to **4**, compound **2** cannot be oxidized reversibly beyond the di(cation radical) state.

Both for **1** and **2** first two electrons are removed at approximately the same potential. This indicates that the two π-segments in **1** and **2** have a small interaction in agreement with the nonresonant nature of the central 1,3-phenylene unit.

UV/Visible/Near-IR and ESR Spectroscopy. UV/visible/near-IR measurements and electron spin resonance (ESR) spectroscopy were applied to obtain information on the electronic transitions and spin states of the various redox states of compounds **1**−**4**. Chemical oxidation of the oligomers was accomplished in dichloromethane with thianthrenium perchlorate ($THI^+ClO_4^-$)[23,24] or with bis(trifluoroacetoxy)iodobenzene (PIFA)[25] in dichloromethane/trifluoroacetic acid (TFA) mixtures. Variable temperature measurements were applied to determine whether the π-dimerization of cation radicals occurs. Before describing the results on the prototype high-spin molecules **1** and **2**, we first consider the model compounds **3** and **4**, which possess only one dopable π-segment.

5,5′-Diphenyl-2,2′-bipyrrole 3. The spectroscopic characterization of the redox states of compound **3** and the π-dimerization of the $\mathbf{3}^{\bullet+}$ cation radical at low temperature have previously been reported in a communication.[17] Here we present a more detailed characterization of the π-dimerization process, obtained by studying the temperature dependence of electronic absorption over a more extended temperature range.

Oxidation of **3** with $THI^+ClO_4^-$ produces the corresponding cation radical $\mathbf{3}^{\bullet+}$, which exhibits two strong absorption bands labeled M1 and M2 at 1.59 and 2.55 eV in the UV/visible/near-IR spectrum (Figure 3a). Each of these two bands is accompanied by additional bands or shoulders at higher energy. Their positions are identical to those previously obtained by electrochemical doping in solution (Table 2).[17] The M1 and

(23) Durand, G.; Morin, G.; Trémillon, B. *Nouv. J. Chem.* **1979**, *7*, 463.

(24) Thianthrenium perchlorate ($THI^+ClO_4^-$) (Shine, H. J.; Dais, C. F.; Small, R. *J. Org. Chem.* **1964**, *29*, 21) was chosen as the oxidizing agent because it combines a relatively high oxidation potential of $E° = 1.23$ V vs SCE with characteristic signals in the UV/visible spectrum ($E = 2.23$ and 4.25 eV) and the ESR spectrum ($g = 2.0081$, $a(H) = 0.132$ mT). The appearance of these signals in the electronic or ESR spectra indicates that further addition of THI^+ does not result in (complete) oxidation of oligothiophene. As an additional advantage, the thianthrene formed in the reduction reaction exhibits an absorption band at $E = 4.83$ eV, well outside the region of interest for the redox states of the present oligothiophenes.

(25) Eberson, L.; Hartshorn, M. P.; Persson, O. *Acta. Chem. Scand.* **1995**, *49*, 640.

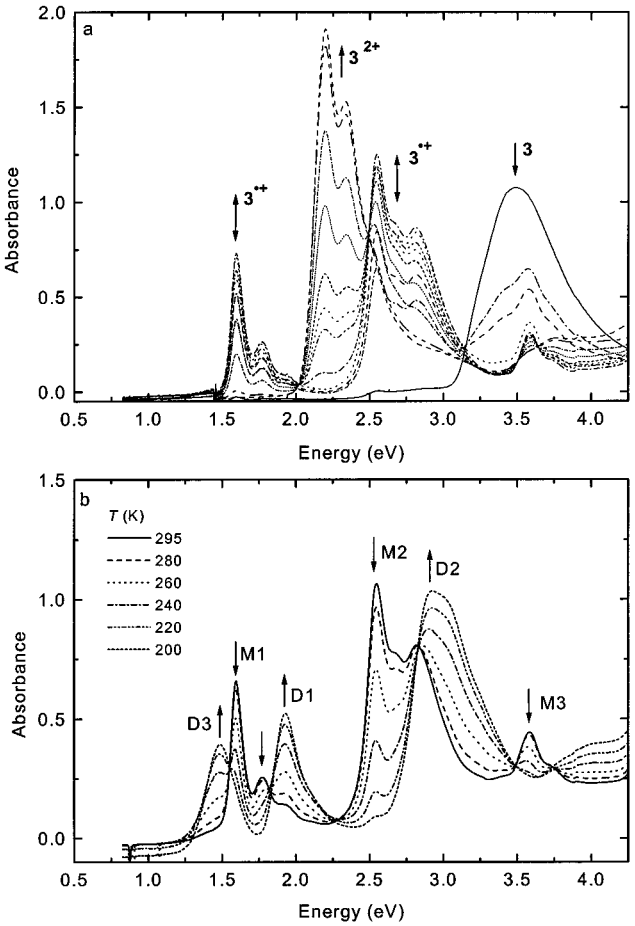

Figure 3. (a) UV/visible/near-IR spectra of **3** as function of the doping level revealing the changes during the redox process **3** → **3**$^{\bullet+}$ → **3**$^{2+}$. (b) UV/visible/near-IR spectra as function of temperature for cation radical **3**$^{\bullet+}$ generated from a 7×10^{-5} M solution of **3** in dichloromethane with $THI^+ClO_4^-$ as oxidizing agent. The temperatures are indicated in the inset. The peaks labeled M1, M2, and M3 are attributed to the monomeric cation radical **3**$^{\bullet+}$, while D1, D2, and D3 are assigned to the cation radical π-dimer **(3)**$_2^{2+}$.

Table 2. Electronic Transitions (eV) of the Redox States of Compounds 1−4[a−c]

compd	N	M1	M2	D1	D2	D3	DC
1	3.40	1.60 (1.77)	2.50	1.91	2.89	1.48	2.23
2	3.25	1.31	2.09	1.61	2.43		
3	3.44	1.59 (1.77)	2.55	1.93	2.92	1.49	2.20 (2.34)
4	3.31	1.34	2.12	1.62	2.55	1.33	

[a] Legend to the labels: N for neutral; M1 and M2 for di(cation radical) (for **1** and **2**) and cation radical (for **3** and **4**); D1, D2, and D3 for π-dimers of di(cation radical) (for **1** and **2**) and of cation radical (for **3** and **4**); DC for di(dication) (for **1** and **2**) and dication (for **3** and **4**). [b] All electronic transitions were determined in dichloromethane solution; concentrations are $\sim 10^{-5}$ M. [c] Values in parentheses are assigned to vibronic peaks of the same electronic transition.

M2 bands have been assigned to dipole-allowed electronic transitions among the frontier orbitals, i.e. the M1 transition corresponds to excitation from the lowest doubly occupied level to the singly occupied level, while M2 involves the excitation from the singly occupied level to the lowest empty level. In addition, a weak band labeled M3 is observed at 3.55 eV. The exact nature of this band is unknown, but it is interesting to note that that correlated calculations performed on short oligo(*p*-phenylene vinylene)s indicate that a positive polaron

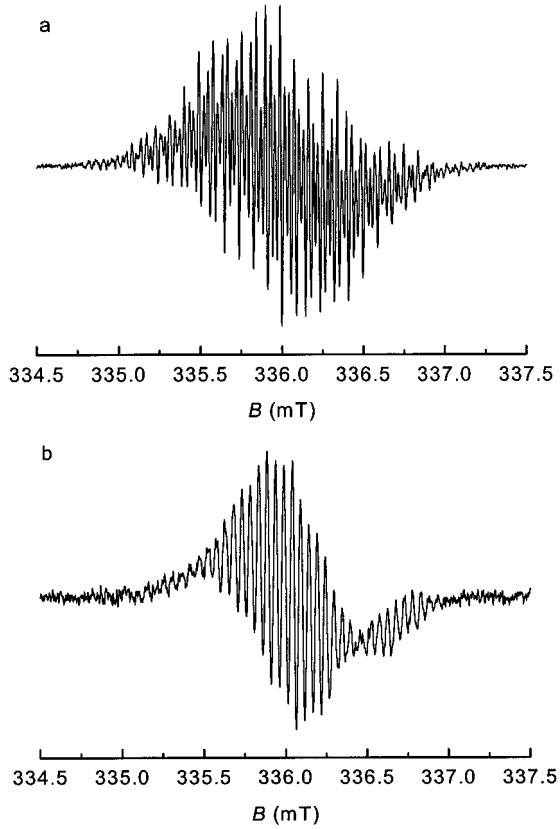

Figure 4. ESR spectra of cation radicals at 295 K. (a) **3**$^{\bullet+}$ oxidized in dichloromethane/TFA. The ESR spectrum can be simulated using the following parameters: $a_H(4H) = 0.614$, $a_H(2H) = 0.853$, $a_H(4H) = 0.382$, $a_H(2H) = 0.703$, $a_H(2H) = 0.395$, $a_H(2H) = 0.470$, and $\Delta H_{pp} = 0.03$ mT. These couplings are tentatively assigned to *o*-PhH, *p*-PhH, *m*-PhH, PyH-3, PyH-4, and NH based on a PM3 quantum chemical calculation. (b) **4**$^{\bullet+}$ oxidized with a $Hg(TFA)_2$ in dichloromethane/TFA.

is characterized not only by two strong subgap absorption features, but also by a third weak absorption peak at an energy higher than that of the neutral band.[26] Upon further oxidation of **3**$^{\bullet+}$ to the dication **3**$^{2+}$, the M1, M2, and M3 bands are replaced by a new absorption at 2.20 eV (DC band) with a vibronic band at 2.34 eV (Figure 3a). Reduction with hydrazine monohydrate revealed that the redox process **3** → **3**$^{\bullet+}$ → **3**$^{2+}$ is reversible on the time scale of the UV/visible/near-IR measurements. The oxidation process is accompanied by an initial increase and subsequent decrease of the well-resolved ESR spectrum of **3**$^{\bullet+}$ (Figure 4a).

Cation radicals **3**$^{\bullet+}$ form π-dimers according to the (reversible) equilibrium: 2 **3**$^{\bullet+}$ ⇄ **(3)**$_2^{2+}$.[17] The π-dimerization equilibrium causes a decrease of the intensity of the ESR spectrum of **3**$^{\bullet+}$ with decreasing temperature, due to the diamagnetic nature of the π-dimer. Figure 3b shows the accompanying changes in the absorption spectrum; the M1 and M2 bands are replaced at lower temperatures by new bands at 1.91 (D1), 2.89 (D2), and 1.48 eV (D3). The D1 and D2 bands are hypsochromically shifted with respect to the M1 and M2 transitions by about 0.3 eV, which is ascribed to a Davydov interaction between the transition dipole moments of the M1 and M2 transitions on the adjacent cation

(26) Cornil, J.; Beljonne, D.; Brédas, J. L. *J. Chem. Phys.* **1995**, *103*, 834.

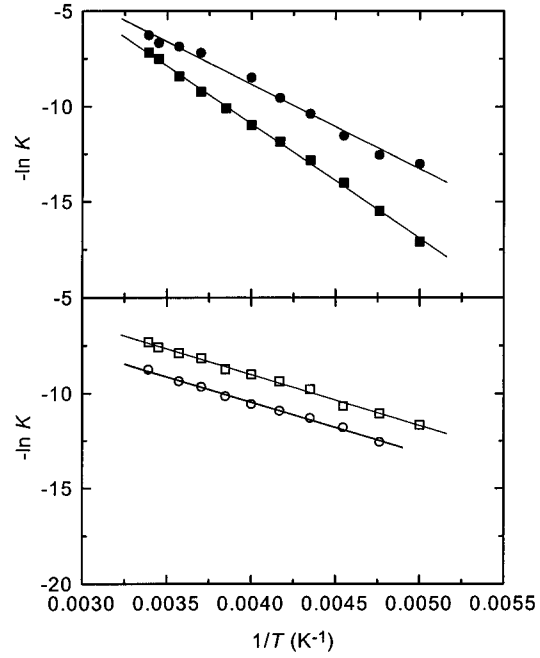

Figure 5. Variation of the π-dimerization constant for the di(cation radicals) of **1** (□) and **2** (○); and the cation radicals **3** (■) and **4** (●) with reciprocal temperature as determined from the temperature variation of the M2 absorptions in the UV/visible/near-IR spectra.

radicals in the π-dimer. The D3 transition, at the lowest energy, is attributed to a charge-transfer transition between the two cation radicals in the π-dimer. The changes with temperature in the ESR spectrum and UV/visible/near-IR spectrum are completely reversible. The M2 transition is well separated from most other absorptions and can be used to estimate the enthalpy of dimerization (ΔH^0_{dim}) by determining the equilibrium constant for dimerization (K = [π-dimer]/[cation radical]^2) as a function of temperature (Figure 5).[27] This analysis gives $\Delta H^0_{dim} = -50$ (±8) kJ/mol and $\Delta S^0_{dim} = -110$ J/mol/K for $\mathbf{3}^{\bullet+}$ in dichloromethane.

5,5′-Diphenyl-2,2′-bithiophene 4. Bithiophene **4** has been oxidized to the cation radical $\mathbf{4}^{\bullet+}$ with PIFA in dichloromethane/TFA. The electronic absorption spectrum of $\mathbf{4}^{\bullet+}$ exhibits two electronic transitions at 1.34 and 2.12 eV, labeled M1 and M2. Further (chemical) oxidation to the dication did not occur because the second oxidation potential of **4** (1.61 V vs SCE) cannot be reached using either PIFA/TFA ($E°$ = 1.30 V vs SCE) or $THI^+ClO_4^-$ ($E°$ = 1.23 V vs SCE).[28] Reduction of $\mathbf{4}^{\bullet+}$ with hydrazine monohydrate afforded **4** quantitatively, demonstrating the full reversibility of the oxidation process. Variable temperature UV/visible/near-IR measurements on $\mathbf{4}^{\bullet+}$ clearly reveal reversible π-dimerization (Figure 6). Upon lowering the temperature, the M1 and M2 bands decrease in favor of the electronic transitions located at 1.62 (D1), 2.56 (D2), and 1.33 eV (D3), belonging to the π-dimer $(\mathbf{4})_2^{2+}$. The assignments of these bands is fully analogous to that of $\mathbf{3}^{\bullet+}$ and $(\mathbf{3})_2^{2+}$.

(27) The normalized absorbance A of the M2 transition can be used to determine K via the relation $K = (1 - A)/(2C_0A^2)$, where C_0 is the total concentration of cation radicals (present as free monomers or incorporated in π-dimers). ΔH^0_{dim} can then be obtained from the slope of a plot of ln K vs $1/T$.

(28) Bard, A. J.; Faulkner, L. R. *Electrochemical Methods*; John Wiley and Sons: New York, 1980; p 702.

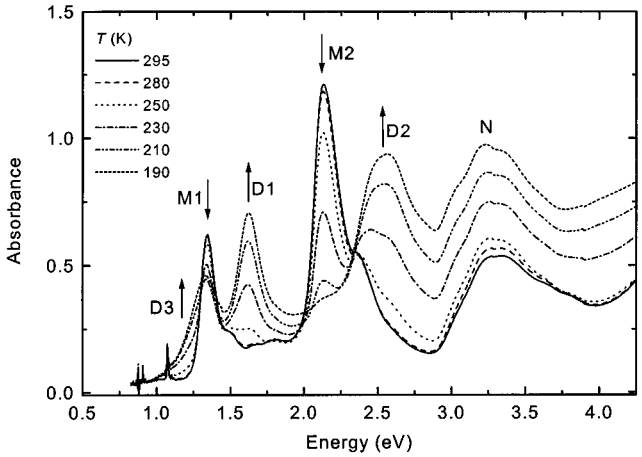

Figure 6. Temperature-dependent UV/visible/near-IR spectra showing the π-dimerization behavior of cation radical $\mathbf{4}^{\bullet+}$ upon decreasing temperature from 295_to 190 K in dichloromethane with THI^+ as oxidizing agent. The peaks labeled M1 and M2 are attributed to the monomeric cation radical $\mathbf{4}^{\bullet+}$, while D1, D2, and D3 are assigned to the cation radical π-dimer $(\mathbf{4})_2^{2+}$; N is a remaining absorption of neutral **4**.

The enthalpy of dimerization estimated from the temperature dependence of the M2 transition is $\Delta H^0_{dim} = -37$ (±8) kJ/mol with $\Delta S^0_{dim} = -75$ J/mol/K (Figure 5).

The cation radical of **4** exhibits a well-resolved ESR spectrum when the oxidation is performed using TFA/mercury trifluoroacetate ($Hg(TFA)_2$) (Figure 4b). The doubly integrated ESR intensity decreases (reversibly) by more than 2 orders of magnitude when the temperature is decreased from 295 to 100 K, supporting the π-dimerization inferred from the electronic absorption spectra.

By using other solvents, other oxidizing agents ($NO^+BF_4^-$), or addition of polymers (polystyrene, poly(ethylene oxide), poly(bisphenol A carbonate), polytetrafluoroethylene, poly(ethylene terephthalate) to make the solution more viscous, we attempted to find conditions that significantly suppress π-dimerization of $\mathbf{4}^{\bullet+}$. However, all these attempts hardly influenced the π-dimerization, and sometimes the addition of polymers made the redox state less stable due to reaction of the polymer with the cation radical. Even the use of solvents with a relatively high melting point, e.g. hexafluoroisopropanol (mp −4 °C) or 1,1,2-trichloroethane (mp −37 °C), did not inhibit the π-dimerization of $\mathbf{4}^{\bullet+}$.

1,3-Bis[5-(5′-phenyl-2,2′-bipyrrolyl)]benzene 1. The evolution of the UV/visible/near-IR spectra of **1** in dichloromethane solution with progressive oxidation is shown in Figure 7. Addition of 2 equiv of $THI^+ClO_4^-$ results in the formation of the di(cation radical) $\mathbf{1}^{2\bullet2+}$, exhibiting absorption bands M1 and M2 at 1.60 and 2.50 eV, respectively (Figure 7). These bands are at the same positions as those for the cation radical of 5,5′-diphenyl-2,2′-bipyrrole ($\mathbf{3}^{\bullet+}$, Table 2). In addition to the M1 and M2 bands a number of other bands and shoulders can be distinguished in the spectrum. Comparison with the low-temperature UV/visible/near-IR spectrum of $\mathbf{3}^{\bullet+}$, strongly suggests that these additional bands are related to π-dimers of an oxidized state of **1**. Further oxidation of $\mathbf{1}^{2\bullet2+}$ results in the di(dication), $\mathbf{1}^{4+}$, exhibiting a strong electronic absorption at 2.23 eV, which replaces the M1, M2, and π-dimer bands of $\mathbf{1}^{2\bullet2+}$. The

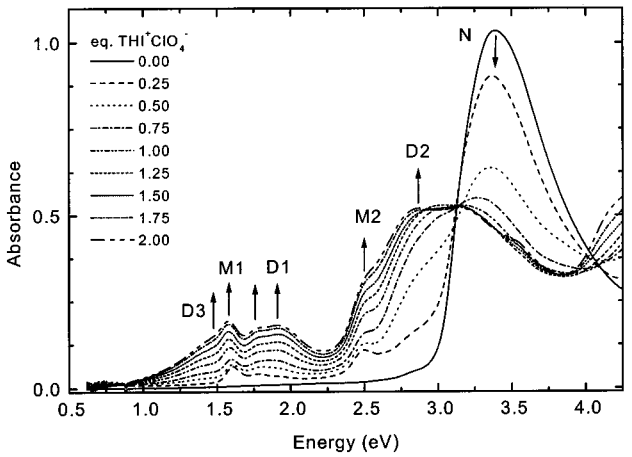

Figure 7. UV/visible/near-IR spectra recorded upon oxidation of neutral **1** to the intermediate oxidation state $\mathbf{1}^{2\bullet 2+}$ via addition of small aliquots of $THI^+ClO_4^-$ to a solution of **1** in dichloromethane. The absorption of neutral **1** is marked with N; the arrows indicate the increase and decrease of various electronic transitions belonging to different redox states.

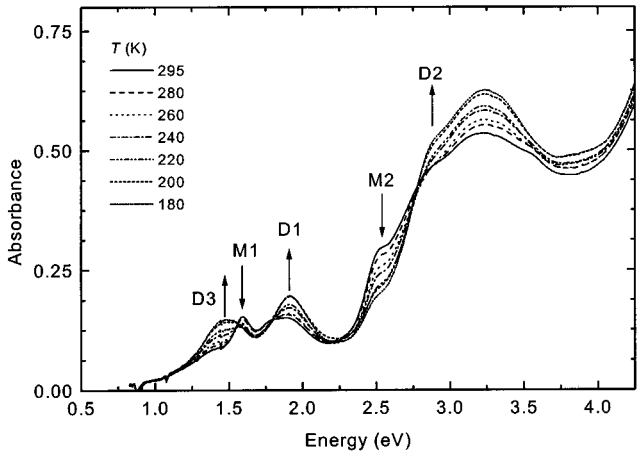

Figure 8. Variable temperature UV/visible/near-IR spectra of $\mathbf{1}^{2\bullet 2+}$ prepared by oxidizing **1** with $THI^+ClO_4^-$. The arrows indicate the changes in electronic transitions upon decrease of the temperature from 295 to 180 K.

position of this new band is at the same energy as for the dication $\mathbf{3}^{2+}$. Apparently, the 1,3-phenylene ring does not seriously affect the electronic absorption spectra of the redox states for **1** as compared to those for **3**, in full accordance with the nonresonant nature of the substitution pattern of the central phenylene ring. Reduction of $\mathbf{1}^{2\bullet 2+}$ with hydrazine monohydrate revealed that the oxidation of **1** is fully reversible on the time scale of the experiments.

The progress of the oxidation has also been followed by combined UV/visible/near-IR−ESR spectroscopy using a dual-purpose cell. The doubly integrated intensity of the unresolved ESR signal reaches a maximum after addition of 2 equiv of $THI^+ClO_4^-$, at the point where the UV/visible/near-IR spectrum corresponds to that of the di(cation radical) $\mathbf{1}^{2\bullet 2+}$. The decrease of the ESR intensity at higher doping levels is due to the formation of higher oxidation states ($\mathbf{1}^{\bullet 3+}$ or $\mathbf{1}^{4+}$).

The maximum ESR intensity at the doubly oxidized level indicates that no strong antiferromagnetic coupling occurs between the two unpaired electrons of $\mathbf{1}^{2\bullet 2+}$. However, this result gives no conclusive information whether ferromagnetic coupling occurs in this diradical, since a similar experimental result is expected for two completely isolated cation radicals. The fact that an ESR signal is observed for this diradical in solution shows that the dipolar interaction between the spins of $\mathbf{1}^{2\bullet 2+}$ is fairly small. In case of a strong dipolar interaction, a short spin lifetime is expected in solution as a result of a modulation of the spin−spin interaction, resulting in undetectably broad lines.[29,30] In general, only for small dipolar splittings, an ESR signal can be detected for a diradical in solution. In that case, a single line will be observed, in absence of resolved hyperfine splitting.

Variable temperature UV/visible/near-IR measurements clearly indicate the formation of π-dimers of the di(cation radical) $\mathbf{1}^{2\bullet 2+}$. The bands M1 and M2 decrease at lower temperatures in favor of the electronic transitions located at 1.48 (D3), 1.91 (D1), and 2.89 (D2) eV (Figure 8). These bands are attributed to π-dimers of the di(cation radical). In accordance with the results for **3** and **4**, this dimerization is fully reversible with temperature. Figures 7 and 8 demonstrate that π-dimerization of $\mathbf{1}^{2\bullet 2+}$ occurs to a significant extent at ambient temperature.

The actual nature of the π-dimers formed for $\mathbf{1}^{2\bullet 2+}$, containing two oxidizable units, can be different from those of $\mathbf{3}^{\bullet +}$, containing only one dopable segment. In principle, both units can interact simultaneously with those of a second di(cation radical) or they may interact with units of two different di(cation radical)s giving rise to multiple π-aggregates instead of simple dimers. In addition, an intramolecular π-association in which the two oxidized units of a single molecule $\mathbf{1}^{2\bullet 2+}$ form a π-dimer-like configuration, cannot be ruled out. The extensive overlap of the various absorption bands (Figure 8) hampers an accurate quantitative analysis of the aggregation in terms of K and ΔH^0_{dim}. Tentative analysis of the temperature dependence of the M2 transition, while assuming a simple dimerization process, suggests $\Delta H^0_{dim} = -22$ (±10) kJ/mol and $\Delta S^0_{dim} = -14$ J/mol/K (Figure 5).[31] The small entropy of dimerization suggests that the π-dimerization of $\mathbf{1}^{2\bullet 2+}$ might be intramolecular, involving the two oxidized units of a single molecule, although such a configuration is sterically unfavorable from molecular models.

Variable temperature ESR measurements performed on the di(cation radical) $\mathbf{1}^{2\bullet 2+}$ show a decrease in doubly integrated ESR intensity at lower temperatures, consistent with π-dimerization. In a frozen matrix at 160 K about half of the ESR intensity remains of $\mathbf{1}^{2\bullet 2+}$ in comparison with room temperature. This is in contrast with the variable temperature ESR measurements performed on cation radical $\mathbf{3}^{\bullet +}$, where almost no ESR signal is observed at 160 K. The different temperature dependence of the ESR intensity for $\mathbf{3}^{\bullet +}$ and $\mathbf{1}^{2\bullet 2+}$ is also reflected in the UV/visible/near-IR experiments presented in Figures 3b and 8. The much smaller decrease

(29) Weissman, S. I. *J. Chem. Phys.* **1958**, *29*, 1189.
(30) Atherton, N. M. *Principle of Electron Spin Resonance*; Ellis Horwood: Chichester, 1993.

(31) For n-merization the relation between K and the normalized absorption A of the M2 transition is $K_n = (1 - A)/(nC_0^{n-1}A^n)$. Plotting of $-\ln K_n$ vs $1/T$ gives a satisfying correlation for $n = 2$ only and fails to give an acceptable correlation for $n > 2$.

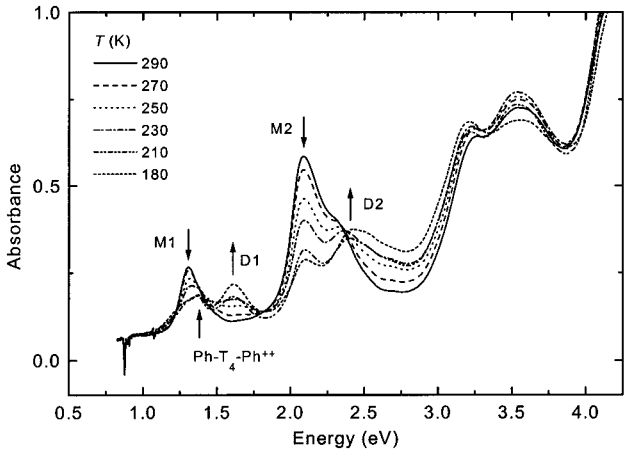

Figure 9. Temperature-dependent UV/visible/near-IR spectra reflecting the π-dimerization behavior of $\mathbf{2}^{2\bullet 2+}$ upon decreasing temperature from 295 to 190 K. The oxidation was performed with $THI^+ClO_4^-$ in dichloromethane. A small feature attributed to the dication of 5,5‴-diphenyl-2,2′:5′,2″:5″,2‴-quaterthiophene ($Ph\text{-}T_4\text{-}Ph^{2+}$), which is present as a small contamination (∼2%), is noted in the spectra at the lowest temperatures.

of the ESR intensity of $\mathbf{1}^{2\bullet 2+}$ with decreasing temperature in comparison with $\mathbf{3}^{\bullet +}$ is in agreement with the lower value of ΔH^0_{dim}, as determined from variable temperature UV/visible/near-IR experiments. We have not observed any splitting of the ESR signal nor a half-field ($\Delta M_s = \pm 2$) signal at lower temperatures that would have indicated the presence of a triplet state for $\mathbf{1}^{2\bullet 2+}$.

5-Methyl-2-dodecyloxy-1,3-bis(5′-[5-phenyl-2,2′-bithiophene])benzene 2. With progressive oxidation, the electronic absorption of **2** at 3.25 eV decreases and two new absorption bands located at 1.31 and 2.09 eV (labeled M1 and M2) emerge. The transitions M1 and M2 are attributed to the cation radical $\mathbf{2}^{\bullet +}$ and the di(cation radical) $\mathbf{2}^{2\bullet 2+}$, based on the close correspondence with the absorption spectrum of $\mathbf{4}^{\bullet +}$ (Table 2). $THI^+ClO_4^-$ is unable to fully convert **2** to the di(cation radical) state $\mathbf{2}^{2\bullet 2+}$, and the characteristic signal of THI^+ appears in the absorption spectrum at $E = 2.23$ eV[24] when the band of neutral **2** has lost a little more than half its intensity. The final degree of oxidation of **2** that can be reached is a little higher when the oxidation is carried out with PIFA in a dichloromethane/TFA mixture (4:1 v/v). In this case less than 20% of N band remains, while the M1 and M2 bands are formed at the same positions as those for the $THI^+ClO_4^-$ oxidation. The redox state $\mathbf{2}^{\bullet +}/\mathbf{2}^{2\bullet 2+}$ is chemically stable, and upon reduction, **2** is recovered quatitatively.

The changes in the absorption spectrum with temperature reveal a fully reversible π-dimerization, similar to the behavior observed for $\mathbf{4}^{\bullet +}$ (Figure 9). The M1 and M2 bands decrease in favor of new absorptions at 1.61 and 2.42 eV, labeled D1 and D2, when the temperature decreases. Analyzing the M2 line intensity of $\mathbf{2}^{2\bullet 2+}$ as a function of temperature and assuming that π-dimers are formed gives $\Delta H^0_{dim} = -22\ (\pm 10)$ kJ/mol and $\Delta S^0_{dim} = -1$ J/mol/K (Figure 5), again suggesting intramolecular π-dimerization.

The broad ESR signal of $\mathbf{2}^{2\bullet 2+}$ decreases in intensity at lower temperature, confirming the π-dimerization of $\mathbf{2}^{2\bullet 2+}$. On the basis of these results it is clear that this π-dimerization inhibits the formation of a triplet state in $\mathbf{2}^{2\bullet 2+}$, similar to the results obtained for $\mathbf{1}^{2\bullet 2+}$.

Conclusions

The possibility to obtain prototype polaronic ferromagnetic diradicals has been investigated using oligomers with two dopable bipyrrole and bithiophene segments linked by 1,3-phenylene. The synthesis of these oligomers was accomplished via palladium-catalyzed aryl−aryl cross-coupling reactions. After extensive purification, including preparative HPLC, the prototype high-spin molecules based on bipyrrole **1** and bithiophene **2** have been obtained. Their redox states have been studied in detail by cyclic voltammetry, UV/visible/near-IR spectroscopy, and ESR spectroscopy at variable temperatures. Compounds **1** and **2** have been oxidized to an intermediate redox state in which both heterocyclic parts carry one unpaired electron, as required for the formation of a high-spin state. Especially for **1** the oxidation process to the di(cation radical) could be performed essentially quantitatively by tuning the amount of oxidizing agent. Variable temperature UV/visible/near-IR and ESR spectroscopy reveal that extensive π-dimerization of these oligo(cation radical)s produces a spinless state, especially at low temperatures. Because of the strong tendency to form π-dimers, it is not possible to obtain high-spin molecules based on dopable π-conjugated segments containing pyrrole or thiophene. The π-dimerization of prototype high-spin oligomers as demonstrated here may also explain the low spin concentrations found in oxidized forms of polymers that were designed to give polaronic ferromagnetic behavior.[12,13]

We conclude that the elegant strategy toward high-spin polymers, using a polaronic ferromagnetic chain in which unpaired electrons can be introduced by reduction or oxidation of dopable π-conjugated segments, suggested by Fukutome et al.[8] is not applicable to the oxidation of oligopyrrole and oligothiophene units. This has important consequences for the design of future polaronic high-spin polyradicals. However, while π-dimerization inhibits the formation of high-spin states in these cases, other π-conjugated ion radicals with a much lesser tendency to form π-dimers, such as *p*-phenylenediamine cation radicals,[10,11] remain interesting building blocks to study intrachain ferromagnetic coupling in polaronic polymer chains.

Experimental Section

General Techniques. All solvents and reagents were reagent grade and used as received. Tetrahydrofuran (THF) and diethyl ether were dried and distilled over sodium/potassium with benzophenone. Dichloromethane was distilled over P_2O_5. For column chromatography Merck silica gel 60 (particle size 0.063-0.200 mm) was used. NMR spectra were recorded on a Bruker AM-400 spectrometer at frequencies of 400.1 and 100.6 MHz for ^1H and ^{13}C nuclei, respectively. Tetramethylsilane (TMS) or THF-d_8 was used as an internal standard for ^1H NMR and $CDCl_3$ for ^{13}C NMR. Infrared (FT-IR) spectra were recorded on a Perkin Elmer 1605 FT-IR spectrophotometer between 4400 and 450 cm^{-1}. Electrospray mass spectra were recorded using a Perkin Elmer-Sciex API 300 MS/MS mass spectrometer. The sample solutions were delivered to the ESMS by a syringe pump (Harvard Apparatus) at a flow rate of ∼5 μL/min. All preparations were performed

under an inert atmosphere. All oxidation experiments were performed under a rigorously inert N_2 atmosphere (<1 ppm H_2O and <10 ppm O_2).

1,3-Bis[*N*-(*tert*-butoxycarbonyl)-2-pyrrolyl]benzene 5. *N*-(*tert*-butoxycarbonyl)-2-(trimethylstannyl)pyrrole[20] (5.0 g, 17.5 mmol) and 1,3-dibromobenzene (2.06 g, 8.7 mmol) were dissolved in a mixture of toluene (60 mL) and a 1 M solution of sodium carbonate in water (60 mL). Tetrakis(triphenylphosphine)palladium(0) (350 mg) was added, and the mixture was stirred for 72 h at 100 °C. After cooling, the resulting solution was extracted with diethyl ether. The combined organic layers were washed with water and dried over magnesium sulfate. Evaporation of the solvent, column chromatography (250 g SiO_2, CH_2Cl_2/hexane (1:3), R_f = 0.30), and recrystallization from hexane afforded **5** as a white solid (1.81 g, 4.43 mmol, 50%). ^{1}H-NMR ($CDCl_3$): δ 7.35 (dd, J = 1.8 and 3.4 Hz, 2H, PyH-5); 7.30-7.20 (m, 4H, PhH); 6.22 (dd, J = 3.4 Hz and 3.5 Hz, 2H, PyH-4); 6.19 (dd, J = 1.8 and 3.5 Hz, 2H, PyH-3); 1.35 (s, 18H, CH_3). ^{13}C-NMR ($CDCl_3$): δ 149.3 (C=O); 134.7 (PyC-2); 133.7 (PhC-1,3); 129.9 (PhC-2/PhC-5); 128.0 (PhC-4,6); 126.6 (PhC-2/PhC-5); 122.5 (PyC-5); 114.3 (PyC-4); 110.5 (PyC-3); 83.5 (*C*-CH_3); 27.5 (C-*C*H_3).

1,3-Bis[*N*-(*tert*-butoxycarbonyl)-5-bromo-2-pyrrolyl]-benzene 6. *N*-bromoscuccinimide (0.35 g, 1.96 mmol) was added to 1,3-bis[*N*-(*tert*-butoxycarbonyl)-2-pyrrolyl]benzene **5** (0.4 g, 0.98 mmol) in THF (10 mL) at −70 °C. After the addition was completed, the mixture was allowed to warm to 0 °C and stirred overnight at 4 °C. Sodium sulfite (0.37 g, 2.94 mmol) was added to the red solution and the solution was stirred for 30 min. After evaporation of the solvent, CCl_4 (75 mL) was added and the resulting suspension was filtered. Evaporation of the solvent yielded pure **6** (0.54 g, 0.97 mmol, 99%). ^{1}H-NMR ($CDCl_3$): δ 7.4−7.2 (m, 4H, PhH); 6.29 (d, J = 3.5 Hz, 2H, PyH-3); 6.16 (d, J = 3.5 Hz, 2H, PyH-4); 1.33 (s, 9H, CH_3). ^{13}C-NMR ($CDCl_3$): δ 148.4 (C=O); 136.0 (PyC-2); 133.8 (PhC-1,3); 127.6 (PhC-2, PhC-5); 127.0 (PhC-4,6); 114.9 (PyC-4); 112.7 (PyC-3); 102.1 (PyC-5); 85.0 (*C*-CH_3); 27.4 (C-*C*H_3).

1,3-Bis[5-[*N*,*N*′-(di-*tert*-butoxycarbonyl)-5′-phenyl-2,2′-bipyrrolyl]]benzene 8. 1,3-Bis[*N*-(*tert*-butoxycarbonyl)-5-bromo-2-pyrrolyl]benzene **6** (0.60 g, 1.06 mmol) and *N*-(*tert*-butoxycarbonyl)-2-phenyl-5-(trimethylstannyl)pyrrole **7**[18] (0.95 g, 2.33 mmol) were dissolved in a mixture of toluene (5 mL) and a 1 M solution of sodium carbonate in water (5 mL). After addition of tetrakis(triphenylphosphine)palladium(0) (25 mg) the mixture was stirred at 100 °C for 96 h. After standard work-up procedures as described for **5**, column chromatography (80 g SiO_2, CH_2Cl_2/hexane (1:3), R_f = 0.20), and recrystallization from hexane, **8** was obtained as an orange solid (0.34 g, 0.38 mmol, 36%) contaminated by small amounts of side products due to homocoupling and debromination. Using preparative HPLC (reversed phase column, eluent acetonitrile/water 9:1) pure **8** was obtained. ^{1}H-NMR ($CDCl_3$): δ 7.44 (t, J = 1.5 Hz, 1H, PhH-2); 7.37−7.28 (m, 13H, PhH-4,6, PhH-5, *o*-PhH, *m*-PhH, *p*-PhH); 6.27 (d, J = 3.3, 2H, PyH-4/PyH-4′); 6.26 (d, J = 3.3, 2H, PyH-4/PyH-4′); 6.24 (d, J = 3.3 Hz, 4H, PyH-3, PyH-3′); 1.27 (s, 18H, CH_3); 1.25 (s, 18H, CH_3). ^{13}C-NMR ($CDCl_3$) δ 149.3 (C=O, C=O′); 136.6, 136.5 (PyC-5, PyC-5′); 134.6, 134.2 (*ipso*-PhC, PhC-1,3); 128.4 (*o*-PhC/*m*-PhC); 128.4, 128.3 (PhC-2, PhC-5); 128.2, 128.1 (PyC-2, PyC-2′); 127.8 (*o*-PhC/*m*-PhC); 127.2 (PhC-4,6); 127.0 (*p*-PhC); 114.5 (PyC-3, PyC-3′); 112.7 (PyC-4, PyC-4′); 83.4 (*C*-CH_3); 27.4 (C-*C*H_3). UV/visible (CH_3CN) λ_{max}: 298 nm. IR (KBr) ν: 2979, 1746, 1369, 1306, 1255, 1149, 848, 789, 752, 699 cm^{-1}. FD-MS ($C_{54}H_{58}N_4O_8$): 891.1 amu (calc), 890.7 amu (found).

1,3-Bis[5-(5′-phenyl-2,2′-bipyrrolyl)]benzene 1. Thermolysis of neat **8** at 190 °C under vacuum for 15 min gave **1** in quantitative yield. ^{1}H-NMR (THF-d_8): δ 10.34 (s, 2H, PyNH/PyN′H); 10.32 (s, 2H, PyNH/PyN′H); 7.85 (t, J = 1.4 Hz, 1H, PhH-2); 7.59 (dd, J = 1.3 and 7.8 Hz, 4H, *o*-PhH); 7.37-7.26 (m, 8H, *m*-PhH, *p*-PhH, PhH-4,6); 7.12 (t, J = 7.4 Hz, 1H, PhH-5); 6.56-6.48 (m, 4H, PyH-3, PyH-4, PyH-3′, PyH-4′). ^{13}C-NMR (THF-d_8): δ 134.7, 134.4 (*ipso*-PhC, PhC-1,3); 132.8, 132.6 (PyC-5, PyC-5′); 129.6 (PhC-5); 129.3 (*m*-PhC); 128.6, 128.5 (PyC-2, PyC-2′); 126.0 (*p*-PhC); 124.2 (*o*-PhC); 121.5 (PhC-4,6); 119.8 (PhC-2); 107.8, 107.7 (PyC-4, PyC-4′); 106.5 (PyC-3, PyC-3′). UV/visible (CH_3CN) λ_{max}: 360 nm.

5,5′-Diphenyl-2,2′-bithiophene 4. 5,5′-Dibromo-2,2′-bithiophene[19] (0.36 g, 1.1 mmol) and trimethylstannylbenzene (0.53 g, 2.20 mmol) were dissolved in a mixture of toluene (7.5 mL) and a 1 M solution of sodium carbonate in water (7.5 mL). After addition of tetrakis(triphenylphosphine)palladium(0) (50 mg) the mixture was stirred at 100 °C for 72 h. The reaction mixture was filtered. The residue was washed with hexane and $CHCl_3$ and dried, yielding pure **4** as a yellow solid (0.23 g, 0.72 mmol, 65%). ^{1}H-NMR (THF-d_8), δ 7.65 (dd, J = 1.1 and 8.4 Hz, 4H, *o*-Ph); 7.39-7.36 (m, 6H, *m*-PhH, ThH-3,3′/ThH-4,4′); 7.26 (tt, J = 1.1 and 7.4 Hz, 2H, *p*-Ph); 7.25 (d, J = 3.9 Hz, 2H, ThH-3,3′/ThH-4,4′). ^{13}C-NMR (THF-d_8): δ 144.0 (ThC-5,5′); 137.8 (ThC-2,2′); 135.0 (*ipso*-PhC); 129.8 (*m*-PhC); 128.4 (ThC-3,3′/ThC-4,4′); 126.2 (*o*-PhC); 125.4 (C-3,3′/C-4,4′); 124.9 (*p*-PhC). UV/visible (CH_3CN) λ_{max}: 371 nm. IR (KBr) ν: 1656, 1636, 1594, 1486, 1446, 1262, 1097, 1022, 797, 751, 686 cm^{-1}.

5-Trimethylstannyl-2,2′-bithiophene 9. *n*-Butyllithium (1.6 M in hexane, 1.6 mL, 2.47 mmol) was added to 2,2′-bithiophene[21] (0.41 g, 2.47 mmol) in THF (10 mL) at -70 °C. The mixture was stirred for 30 min. After addition of trimethyltin chloride (0.49 g, 2.47 mmol) in THF (15 mL) the mixture was stirred for 45 min at -70 °C and overnight at ambient temperature. The yellow solution was poured into water and extracted with diethyl ether. The combined organic layers were washed with water and dried over magnesium sulfate. Evaporation of the solvent afforded **9** as a green oil (0.69 g, 2.10 mmol, 85%). ^{1}H-NMR (CD_3CN): δ 7.15 (d, J = 3.3 Hz, 1H, ThH-4); 7.10 (dd, J = 1.0 and 5.1 Hz, 1H, ThH-5′); 7.05 (dd, J = 1.0 and 3.7 Hz, 1H, ThH-3′); 6.98 (d, J = 3.3 Hz, 1H, ThH-3); 6.87 (dd, J = 3.7 and 5.1 Hz, 1H, ThH-4′); 0.27 ($Sn(CH_3)_3$). ^{13}C-NMR (CD_3CN): δ 143.4 (ThC-5); 138.8, 138.2 (ThC-2, ThC-2′); 135.8 (ThC-4); 127.7 (ThC-5′); 125.0, 124.1, 123.5 (ThC-3, ThC-3′, ThC-4′); −8.2 ($Sn(CH_3)_3$).

5-Phenyl-2,2′-bithiophene 10. 5-Trimethylstannyl-2,2′-bithiophene **9** (0.69 g, 2.10 mmol) and bromobenzene (0.33 g, 2.10 mmol) were dissolved in a mixture of toluene (10 mL) and a 1 M solution of sodium carbonate in water (10 mL). After addition of tetrakis(triphenylphosphine)palladium(0) (50 mg), the mixture was stirred at 100 °C for 48 h. After standard work-up procedures as described for **5**, column chromatography (40 g SiO_2, CH_2Cl_2/hexane (1:7), R_f = 0.3), and recrystallization from hexane, **10** was obtained as a yellow solid (0.25 g, 1.03 mmol, 50%). ^{1}H NMR ($CDCl_3$): δ 7.61 (dd, J = 1.3 and 7.3 Hz, 2H, *o*-PhH); 7.38 (dd, J = 7.3 and 7.3 Hz, 2H, *m*-PhH); 7.28 (tt, J = 1.3 and 7.3 Hz, 1H, *p*-PhH); 7.23-7.20 (m, 3H, ThH-3/ThH-4, ThH-3′, ThH-5′); 7.15 (d, J = 3.7 Hz, ThH-3/ThH-4); 7.03 (dd, J = 3.7 and 5.1 Hz, 1H, ThH-4′). ^{13}C-NMR ($CDCl_3$): δ 143.1 (ThC-5); 137.4, 136.7 (ThC-2, ThC-2′); 134.0 (*ipso*-PhC), 128.9 (*m*-PhC), 127.8 (ThC-5′), 125.6 (*o*-PhC), 127.6, 124.6, 124.4, 123.7, 123.6 (*p*-PhC, ThC-3, ThC-4, ThC-3′, ThC-4′).

5′-Trimethylstannyl-5-phenyl-2,2′-bithiophene 11. *n*-Butyllithium (1.6 M in hexane, 0.65 mL, 1.04 mmol) was added to 5-phenyl-2,2′-bithiophene **10** (0.25 g, 1.03 mmol) in THF (10 mL) at −70 °C. Subsequently, trimethyltin chloride (0.21 g, 1.06 mmol) in THF (2 mL) was added, and the mixture was warmed to ambient temperature. Work-up analogous to **9** afforded **11** as a yellow solid (0.42 g, 1.03 mmol, 100%). ^{1}H-NMR ($CDCl_3$): δ 7.59 (dd, J = 1.4 and 7.4 Hz, 2H, *o*-PhH); 7.36 (dd, J = 7.4 and 7.4 Hz, 2H, *m*-PhH); 7.30 (d, J = 3.4 Hz, 1H, ThH-4′); 7.28 (tt, J = 1.4 and 7.4 Hz, 1H, *p*-PhH); 7.21 (d, J = 3.9 Hz, 1H, ThH-3); 7.13 (d, J = 3.9 Hz, 1H, ThH-4); 7.10 (d, J = 3.4 Hz, 1H, ThH-3′); 0.41 (s, 9H, $Sn(CH_3)_3$). ^{13}C-NMR ($CDCl_3$): δ 142.9, 142.8 (ThC-5, ThC-5′); 137.5, 136.8 (ThC-2, C-2′); 135.9 (ThC-4′); 134.1 (*ipso*-PhC); 128.9 (*m*-PhC); 127.4 (*p*-PhC); 125.5 (*o*-PhC); 124.8, 124.2, 123.7 (ThC-3, ThC-4, ThC-3′); -6.4 ($Sn(CH_3)_3$).

5-Methyl-2-dodecyloxy-1,3-dibromobenzene 12. Potassium carbonate (5.2 g, 37.6 mmol) and dodecylbromide (1.88 g, 7.5 mmol) were added to 2,6-dibromo-4-methylphenol (2.0 g, 7.5 mmol) in DMF (20 mL). The reaction mixture was stirred overnight at 60 °C and poured into diethyl ether. The

organic layer was washed with water and diluted HCl solution and dried over magnesium sulfate. Evaporation of the solvent afforded **12** (3.0 g, 6.9 mmol, 92%) as a yellow oil. ^{1}H-NMR ($CDCl_3$): δ 7.29 (s, 2H, PhH-4,6); 3.95 (t, J = 6.5 Hz, 2H, OCH_2); 2.26 (s, 3H, $PhCH_3$); 1.85 (q, J = 7.0 Hz, 2H, OCH_2CH_2); 1.52 (q, J = 6.9 Hz, 2H, $OCH_2CH_2CH_2$); 1.32 (m, 16H, dodecyl-CH_2); 0.88 (t, J = 7.0 Hz, 3H, dodecyl-CH_3); ^{13}C-NMR ($CDCl_3$): δ 151.2 (PhC-2); 136.1 (PhC-5); 133.0 (PhC-4,6); 117.9 (PhC-1,3); 73.5 (O-CH_2); 31.9 ($CH_2CH_2CH_3$); 30.0-29.4 (dodecyl-C), 25.9 ($OCH_2CH_2CH_2$); 22.7 (CH_2CH_3); 20.2 ($PhCH_3$), 14.1 (CH_2CH_3).

5-Methyl-2-dodecyloxy-1,3-bis(5′-[5-phenyl-2,2′-bithiophene])benzene 2. Tetrakis(triphenylphosphine)palladium-(II) chloride (50 mg) was added to 5-methyl-2-dodecyloxy-1,3-dibromobenzene (0.86, 2.0 mmol) and **10** (1.60, 4.0 mmol) in THF (20 mL). The reaction mixture was refluxed for 24 h. Work-up procedures as described for **5**, followed by column chromatography (300 g SiO_2, hexane, R_f = 0.25), and recrystallization from ethanol afforded **2** (0.15 g, 0.2 mmol, 10%) as yellow crystals. Compound **2** was purified using preparative HPLC (reversed phase column, eluent THF/water 3:1). ^{1}H-NMR (THF-d_8): δ 7.65 (dd, J = 1.5 and 7.5 Hz, 4H, *o*-PhH); 7.50 (d, J = 3.8 Hz, 2H, ThH-4′); 7.43 (s, 2H, PhH-4,6); 7.38 (dd, J = 7.5 and 7.5 Hz, 4H, *m*-PhH); 7.37 (d, J = 3.8 Hz, 2H, ThH-4); 7.27 (tt, J = 1.5 Hz and 7.5 Hz, 2H, *p*-PhH); 7.27 (d, J = 3.8 Hz, 4H, ThH-3, ThH-3′); 3.65 (t, J = 7.0 Hz, 2H, OCH_2); 2.39 (s, 3H, $PhCH_3$); 1.83 (q, J = 7.0 Hz, 2H, OCH_2CH_2); 1.35 (q, J = 7.0 Hz, 2H, $OCH_2CH_2CH_2$); 1.20 (m, 16H, dodecyl-H); 0.84 (t, J = 7.0 Hz, 3H, CH_2CH_3). ^{13}C-NMR (THF-d_8): δ 151.2 (PhC-2); 143.9 (ThC-5); 138.9 (ThC-5′); 138.7 (PhC-5); 137.7 (ThC-2, ThC2′); 135.1 (*ipso*-Ph); 129.8 (*m*-PhC); 129.5 (PhC-4,6); 129.3 (PhC-1,3); 128.3; 127.8 (ThC-3, ThC-3′); 126.2 (*o*-PhC); 125.2; 124.3 (ThC-4, ThC-4′); 124.8 (*p*-PhC); 74.3 (OCH_2); 32.9 ($CH_2CH_2CH_3$); 31.2−30.3 (dodecyl-CH_2); 26.8 (OCH_2-CH_2CH_2); 23.5 (CH_2CH_3); 20.9 ($PhCH_3$); 14.4 (CH_2CH_3). EI-MS ($C_{47}H_{48}OS_4$): 756.3 amu (calc), 756.0 amu (found).

Cyclic Voltammetry. Cyclic voltammograms were recorded in dichloromethane with 0.1 M tetrabutylammonium hexafluorophosphate ($Bu_4N^+PF_6^-$) as supporting electrolyte using a Potentioscan Wenking POS73 potentiostat. The working electrode was a platinum disc (0.2 cm^2), the counter electrode was a platinum plate (0.5 cm^2), and a saturated calomel electrode was used as reference electrode, calibrated against a Fc/Fc^+ couple (+0.43 V vs SCE). Typical concentration of the substrates in cyclic voltammetry experiments was 10^{-3} M.

UV/Visible/Near-IR. UV/visible/near-IR experiments (200-3300 nm) were recorded with a Perkin Elmer Lambda 900 spectrophotometer with path lengths of 1 or 10 mm. Oxidation experiments were carried out by adding oxidant solution via a gas-tight Hamilton syringe through a Teflon-lined septum sealing the cuvette under magnetic stirring of the substrate solution. Variable temperature experiments down to 80 K were done with an Oxford Optistat continuous flow cryostat and an Oxford ITC 502 controller in 10 K steps. The samples were allowed to reach equilibrium at each temperature for 3 min before recording a scan. During the equilibration and the scan the temperature remained constant within ±0.3 K.

ESR. ESR spectra were recorded with an X-band Bruker ESP 300E spectrometer, operating with a standard or TMH cavity, an ER 035M NMR Gauss meter, and a HP 5350B frequency counter. Temperature was controlled via a Bruker ER 4111 variable temperature unit between 100 and 300 K. The temperature remained constant within ±1 K. Variable temperature ESR experiments in dichloromethane were done with a flat cell. Combined UV/visible/near-IR and ESR studies were performed with a homemade cell consisting of a 10 mm quartz cuvette, a quartz 4 mm o.d. ESR tube, and a Teflon-lined septum-sealed entry port for addition of oxidizing agent using a gas-tight Hamilton syringe. For determining the signal intensity, the ESR spectra were doubly integrated after baseline correction.

Acknowledgment. We thank Mr. J. L. J. van Dongen for assistance with preparative HPLC and Ms. J. J. Apperloo for recording some of the UV/visible/near-IR spectra. Prof. E. W. Meijer, Dr. M. M. Wienk, Dr. J. A. J. M. Vekemans, and Dr. E. E. Havinga are acknowledged for stimulating discussions and valuable comments. Philips Research is gratefully acknowledged for an unrestricted research grant.

Supporting Information Available: UV/visible/near-IR spectra at various oxidation levels for **1**, **2**, and **4** (4 pages). See any current masthead page for ordering information and Internet access instructions.

CM970759I